Relationship Between the Material Properties and Fatigue Crack-Growth Characteristics of Natural Rubber Filled with Different Carbon Blacks

Yijing Nie, Bingyin Wang, Guangsu Huang, Liangliang Qu, Peng Zhang, Gengsheng Weng, Jinrong Wu

State Key Laboratory of Polymer Materials Engineering, College of Polymer Science and Engineering, Sichuan University, Chengdu 610065, People's Republic of China

Received 30 September 2009; accepted 16 January 2010
DOI 10.1002/app.32098
Published online 12 May 2010 in Wiley InterScience (www.interscience.wiley.com).

ABSTRACT: An investigation of the influence of different types of carbon black on fatigue crack-growth behavior was undertaken. Fatigue tests were carried out on edge-notched specimens under cyclic tension loading. A power-law dependency between the crack-growth rate and tearing energy was obtained. Natural rubber (NR) filled with N330 (the mean diameter is 30 nm) carbon black possessed the lowest values of exponent b and constant B (the two crack growth parameters determined from cyclic crack growth testing), which denoted the strongest resistance to crack growth at a given tearing energy. Strain-induced crystallization was investigated by the modified Mooney–Rivlin equation and showed the earliest appearance and strongest ability of the crystallization of the NR/N330 composite at the largest amount of bound rubber. The study on the viscoelastic properties by dynamic mechanical analysis confirmed that the NR/N330 composite had the largest viscoelastic contribution, which was attributed to the viscoelastic dissipation in the viscoelastic region in front of the crack tip. All of these results confirm the best crack-propagation resistance of NR filled with N330. © 2010 Wiley Periodicals, Inc. J Appl Polym Sci 117: 3441–3447, 2010

Key words: crazing; crystallization; fatigue analysis; rubber; viscoelastic properties

INTRODUCTION

Natural rubber (NR), because of its outstanding mechanical properties, large elastic deformation, and good crack-growth resistance, is widely used in industry. To improve the structural and thermal properties to meet the needs of practical applications, fillers are commonly used. Carbon black represents the predominant class of reinforcing fillers in the rubber industry. There are various kinds of carbon blacks, whose diameter, structure, and specific surface area differ.[1] In practice, NR products may rupture after some cycles of mechanical loading, which results from the propagation of intrinsic flaws within them. To ensure the service security and predict the fatigue lives of these rubber products, which frequently suffer from cyclic loading, the study of the fatigue behavior of rubber reinforced by different carbon blacks becomes important and crucial.

Now, two fatigue analysis approaches exist: the crack-nucleation approach and the crack-growth approach.[2] The crack-growth approach explicitly considers preexisting flaws on the basis of fracture mechanics. Griffith[3] proposed that crack growth is due to the conversion of a structure's stored potential energy to surface energy associated with new crack surfaces. Thomas[4] and Lake and Lindley[5] extended the approach further to investigate crack growth under cyclic loading in NR. A power-law relationship between the crack-growth rate (dc/dn) and the peak energy release rate [i.e., the tearing energy (T)] was discovered.

Because of the intrinsic flaws existing in rubber composites, crack-growth behavior is an important factor determining the strength and durability of rubber. Dizon et al.[6] and Kim and Jeong[7] investigated the influence of different carbon blacks on the fatigue properties of NR, concluding that the fineness and structure of carbon black are two important factors in determining fatigue life, which decreased obviously with finer carbon blacks but increased with larger structure carbon blacks. Lake and Lindley[8] reported that dc/dn decreased with the addition of carbon black. Chung et al.[9] noticed that T became

Correspondence to: G. Weng (guangsu-huang@hotmail.com).

Contract grant sponsor: National Natural Science Foundation of China; contract grant number: 50673059.
Contract grant sponsor: National Basic Research Program of China; contract grant number: 2007CB714701.

maximal around a loading of 40 phr in styrene–butadiene rubber and NR. Apparently, the addition of carbon black changes the local deformation,[10] network structure,[11] dynamic properties[12] and micromorphology evolution during deformation[13] of rubber composites, all of which directly affect and even dominate the fatigue properties and crack-propagation behavior. However, little attention has been paid to collating all of these effects to study the relationship between carbon black and the crack-growth characteristics of NR. Thus, in this study, the relationship between fatigue crack-growth behavior and the effect of different types of carbon black on the rubber properties, including strain amplification, filler network, rubber–filler interactions, dynamic mechanical properties, and strain-induced crystallization, were examined.

EXPERIMENTAL

Materials

Pure NR and NR filled with two kinds of carbon black, N330 (the mean diameter is 30 nm) and N770 (the mean diameter is 70 nm) were studied. The NR used was ribbed smoked sheet no. 1 from Perubahan terbaru Perkebunan Nusantara II (PTPN II, Medan, Sumatra Utara, Indonesia). N330 and N770 were purchased from China Rubber Group Carbon Black Research & Design Institute (Zigong, Sichuan, China). The recipes of these composites are listed in Table I, and the characteristics of the two kinds of carbon black are shown in Table II.

Cyclic loading testing

Fatigue tests were conducted on edge-notched prismatic specimens, the dimensions of which were in accordance with that used by Schubel et al.[14] The specimens had a gage length of 89.0 mm, a width of 25.4 mm, a thickness of 2.0 mm, and an initial crack of length of around 5.0 mm cut into the edge of the rubber specimens by a sharp razor blade. The specimens were subjected to tension–tension fatigue testing with a displacement-controlled mode in MTS810 at room temperature. The displacement was prescribed as a sinusoidal pulse at a frequency of 3 Hz with a maximum strain of 0.2 and an R ratio (R ratio is defined as the ratio of minimum to maximum deformation of rubber during cycles of 0). During the tests, the machine was periodically stopped to record the number of cycles and the length of the crack as measured by a digital camera. For the Mullins effect, the samples were stretched to a predetermined elongation of 200% by cycling three times.

TABLE I
Recipes of NRs Filled with Different Carbon Blacks

Ingredient	Content (phr)		
NR	100	100	100
Stearic acid	2	2	2
Zinc oxide	5	5	5
N-(1,3-dimethylbutyl)-*N*′-phenyl-*p*-phenylenediamine (antioxidant 4020)	1	1	1
N-Cyclohexyl-2-benzothiazole sulfonamide	0.8	0.8	0.8
Tetramethyl thiuram disulfide	0.6	0.6	0.6
Sulfur	1	1	1
N330	30	15	
N770		15	30

TABLE II
Material Characteristics of the Different Carbon Blacks

Filler	Particle size (nm)	Nitrogen absorption (m^2/g)	*n*-dibutyl phthalate (DBP) absorption ($cm^3/100$ g)
N330	28–36	83	102
N770	61–100	27	70

Content of the bound rubber

The method reported by Leblanc and Hardy[15] was used to determine the amount of bound rubber. The amount of bound rubber in weight percentage of the initial rubber content of the compound is given by the following equation:

$$\text{Bound rubber } (\%) = [(m_0 - m_1)/m_0] \times 100 \quad (1)$$

where m_0 is the rubber content in the sample and m_1 is the rubber content extracted by toluene over 72 h at room temperature.

Dynamic mechanical analysis (DMA)

The viscoelastic characteristics of the samples were measured through DMA in tension mode at a frequency of 1 Hz in a broad temperature range of −80 to 20°C with a Q800 dynamic mechanical spectrum device of TA Corp (New Castle, Delaware). For the Payne effect, samples were measured at room temperature at 1 Hz in the dynamic strain range 0–20%.

RESULTS AND DISCUSSION

T, which drives the crack at a given rate, is expressed as

$$T = -\frac{\partial U}{\partial A} \quad (2)$$

where U is the total elastic strain energy stored in the component and A is the area of one fracture surface of the crack. Four distinct regimes of fatigue

crack-growth behavior based on various energy release rates have been found under cyclic tensile loading with a zero stress ratio.[5] In regime 1, T remains below a threshold (T_0), and dc/dn proceeds at a small and constant rate:

$$dc/dn = r, T \leq T_0 \tag{3}$$

where r is a small and constant crack growth rate. Nevertheless, the values of dc/dn become infinite when T is higher than a critical value (T_c), at which the fast fracture of the sample takes place (regime 4). In regime 2, the fatigue dc/dn value of rubber increases linearly with increasing energy release rate:

$$dc/dn = A(T - T_0) + r, T \leq T_t \tag{4}$$

where T_t is a transition value between T_0 and T_c and A represents a fatigue parameter and should be determined experimentally. After the transition region, there is a range between T_t and T_c, over which the relationship between dc/dn and the energy release rate obeys a power law (regime 3):

$$dc/dn = BT^b, T_t \leq T \leq T_c \tag{5}$$

In a simple tension specimen with a single edge cut, T depends on the gauge section strain energy density (W), the size of the crack (c), and a strain-dependent parameter (k):[2]

$$T = 2kWc \tag{6}$$

Lake[16] proposed an approximate relation for k:

$$k = \frac{\pi}{\sqrt{\lambda}} \tag{7}$$

where λ is the extension ratio.

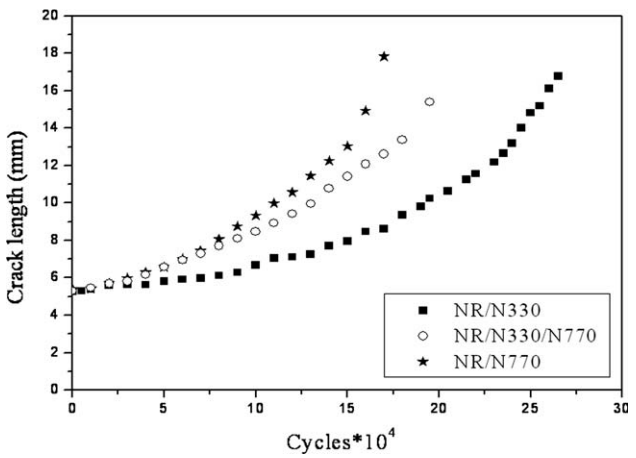

Figure 1 Crack length versus the fatigue cycles for the rubber composites.

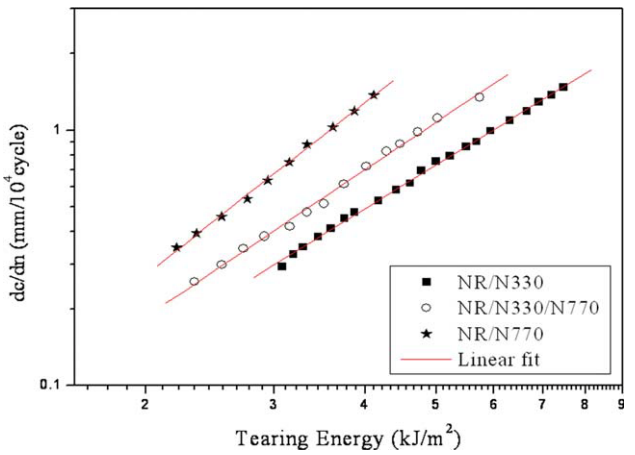

Figure 2 dc/dn versus T. [Color figure can be viewed in the online issue, which is available at www.interscience.wiley.com.]

Thus, T of a rubber sample containing a crack under uniaxial stretching could be determined as follows:

$$T = 2\pi\lambda^{-1/2}Wc \tag{8}$$

In this condition, dc/dn with the energy release rate can be expressed for regime 3 as follows:

$$dc/dn = B(2\pi\lambda^{-1/2}Wc)^b \tag{9}$$

Figure 1 shows the crack growth versus fatigue cycle plots for specimens filled with different carbon blacks. dc/dn was determined from the incremental change in the crack length to the corresponding increase in number of cycles, and the T values were determined from eq. (8) at different crack lengths.[17] Figure 2 displays the relationship between dc/dn and T on a logarithmic scale, which obeyed a power-law dependency (regime 3). The fatigue parameters are listed in Table III. The lower values of exponent b and constant B for the NR filled with N330 denoted a stronger resistance to crack growth at a given T value compared with the rubbers filled with other carbon blacks. The exponent b and constant **B** are the two crack growth parameters determined from cyclic crack growth testing.

The nonlinear viscoelastic behavior versus strain was investigated, and a strong reduction in the storage modulus associated with the Payne effect was found, as shown in Figure 3. The storage modulus

TABLE III
Fatigue Parameters of the Rubber Composites Filled with Different Carbon Blacks

Composite	B	b
NR/N330	0.0429	1.76
NR/N330/N770	0.0491	1.92
NR/N770	0.0574	2.24

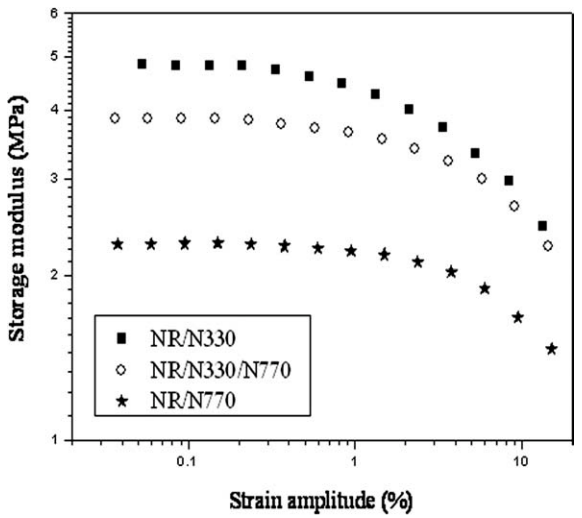

Figure 3 Storage modulus versus the dynamic strain amplitude for the filled rubbers.

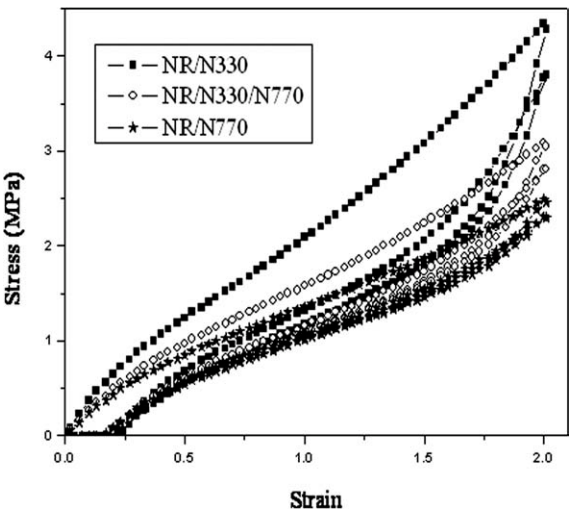

Figure 4 Mullins effect of the rubber composites.

was highest at a small amplitude (E_0') and then monotonically decreased to a low value (E_∞'). The modulus plateau was not reached at a high dynamic strain amplitude because of the strain limitation of the device. As shown in Figure 3 and Table IV, NR reinforced by N330 showed a stronger magnitude of the Payne effect and indicated more powerful filler–filler interactions or a more perfect filler network in the rubber matrix.[18,19] Figure 4 shows the influence of the carbon black on the Mullins effect. To quantifiably reveal the Mullins effect of the rubbers filled with different carbon blacks, the *Mullins hysteresis*,[20] defined as the area between the first and second extension, was calculated to reveal the magnitude of the Mullins effect. The higher Mullins hysteresis of the rubber filled with N330 revealed stronger rubber–filler interactions and energy dissipation.[21] On the one hand, the presence of strong filler–filler and rubber–filler interactions, confirmed by the magnitude of the aforementioned Payne and Mullins effects, enhanced the rubber network and, simultaneously, the resistance to crack propagation. On the other hand, the large energy dissipation led to a small stored elastic strain energy in NR, which drove the growth of crack. As a result, the rate of crack growth decreased. The rubber filled with N330, which had smaller particle size and larger structure (Table II), had more intensive filler–filler and rubber–filler interactions, a bigger energy dissipation during stretching, and consequently, a stronger resistance to crack growth. Correspondingly, the rubber filled with N770, which had less intensive filler–filler and rubber–filler interactions and a smaller energy dissipation during stretching, which resulted from its bigger particle size and lower structure, possessed the worst crack-growth resistance.

Moreover, the addition of carbon black changes the viscoelastic properties, local deformation, and strain-induced crystallization at the crack tip of rubber, all of which greatly affect the crack-propagation behavior. The energy dissipation at a crack, according to T in rubbery materials, has two contributions.[22] The first contribution is associated with the energy necessary to break the bonds at the crack tip, and the second contribution is attributed to the viscoelastic dissipation in the linear viscoelastic region in front of the crack tip (Fig. 5). Because strain can induce crystallization in NR, the innermost region at the crack tip can be crystallized during stretching because of the stress concentration and strain amplification of the crack[23,24] (the dark

TABLE IV
Magnitude of the Payne Effect for the Rubber Composites Filled with Different Carbon Blacks

Composite	E_0' (MPa)	E_∞' (MPa)	$E_0' - E_\infty'$ (MPa)	Mullins hysteresis (MPa)
NR/N330	4.85	2.45	2.40	1.47
NR/N330/N770	3.86	2.26	1.60	0.81
NR/N770	2.27	1.47	0.80	0.57

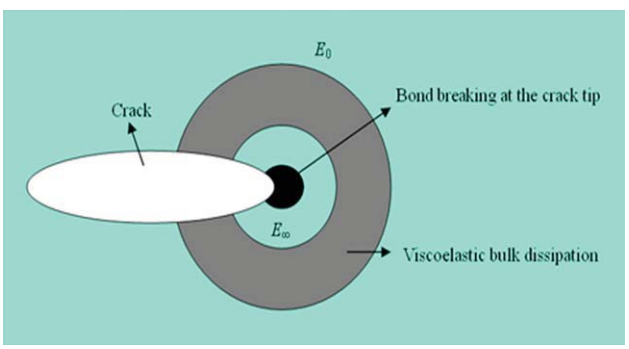

Figure 5 Two contributions of the crack-propagation energy. [Color figure can be viewed in the online issue, which is available at www.interscience.wiley.com.]

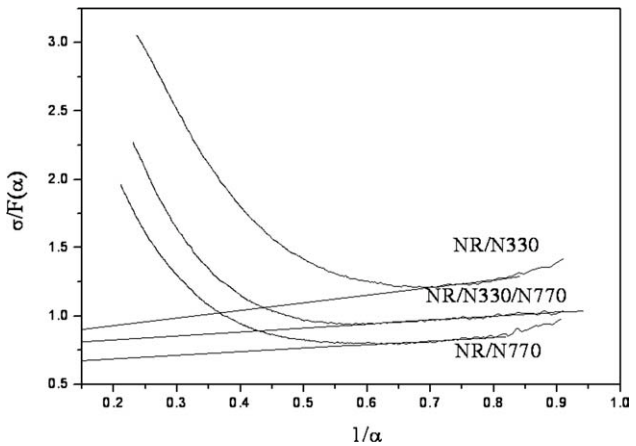

Figure 6 Modified Mooney–Rivlin plots for the rubber composites.

area at the crack tip in Fig. 5). The real strain in the crack tip has some corresponding relationships with the bulk, both of which are influenced by the addition of filler. Namely, the stronger ability and earlier onset of strain-induced crystallization in the bulk result in a greater area of the crack tip crystallization zone and an improvement of its crystallinity.[23]

The upturn in the stress–strain plot of rubber is attributed to the limitation of extensibility of the rubber chains and the strain-induced crystallization. However, these two effects cannot be separated by the original Mooney–Rivlin equation. To only investigate the strain-induced crystallization, the effect of the finite extensibility of elastomer chains must be eliminated. At the high extension, the Gaussian distribution will not hold because the rubber chains are approaching their maximum extension. James and Guth[25] proposed a new constitutive equation of rubber elasticity to deal with the stress–strain behavior of highly extended rubber, which was based on non-Gaussian conformation statistics with the inverse Langevin statistic function of fractional elongation: α/α_m (where α is the elongation ratio and α_m is the maximum elongation ratio, i.e., α at break point in the stress–strain plots). Therefore, the new deviation at the large extension between the stress–strain curve and the James and Guth model should be only attributed to strain-induced crystallization. Subsequently, on the basis of a similar idea, Furukawa et al.[26] put forward a simplified modified Mooney–Rivlin equation as follows:

$$\sigma = 2(C_1 + C_2\alpha^{-1})F(\alpha) \tag{10}$$

where σ is the force divided by the undeformed cross-sectional area and C_1 and C_2 are the Mooney–Rivlin constants, which are independent of the extension ratio (α). $F(\alpha)$ is a deformation function given by

$$F(\alpha) = \frac{\alpha_m}{2}\ln\frac{1+\alpha/\alpha_m}{1-\alpha/\alpha_m} - \frac{1}{\alpha^2} \tag{11}$$

where α_m is the maximum extension ratio, that is, α at the breakpoint in the stress–strain curve. The upturn at high strain in the modified stress–strain curves is attributed to the effect of strain-induced crystallization.[27]

Equation (11) can be expanded to

$$F(\alpha) = \alpha - \frac{1}{\alpha^2} + \frac{\alpha_m}{3}\left(\frac{\alpha}{\alpha_m}\right)^3 + \ldots \tag{12}$$

Equation (10) can be transformed to

$$\frac{\alpha}{\alpha - 1/\alpha^2} \cong 2(C_1 + C_2/\alpha)\left(1 + \frac{1}{3}\frac{\alpha^2}{\alpha_m^2}\right) \tag{13}$$

This equation possesses an extreme point, namely, the upturn in the modified Mooney–Rivlin equation plot at a condition of

$$d\alpha/\left(\alpha - 1/\alpha^2\right)/d\alpha = 0 \tag{14}$$

Then, the critical value of the strain, at which the strain-induced crystallization appears (α_u), can be given by

$$\left(\frac{1}{\alpha_u}\right)^3 = \frac{2C_1}{3\alpha_m^2 C_2} \tag{15}$$

The $\alpha/F(\alpha)$ versus $1/\alpha$ plots of the filled rubbers are shown in Figure 6, and the values of C_1, C_2, and α_u calculated by the modified Mooney–Rivlin equation are listed in Table V. The N330-filled rubber displayed the largest value of C_1, which was dependent on the crosslinking density and the modulus of the rubber; this indicated the strongest reinforcing effect of N330 on rubber and the most powerful filler–rubber interactions in this rubber composite. The lowest value of α_u listed in Table V demonstrated that the N330-filled NR crystallized at the lowest strain. In fact, according to the pioneer work by Poompradub et al.,[28] when the amount of bound rubber is larger, the strain-induced crystallization will occur at smaller strain. Because the bound rubber,[29,30] which strongly adheres to the particle surface, cannot deform under the action of the external stress, the effective strain ratio of the rubber portion is much larger than the macroscopic one; that is, the strain

TABLE V
Onset of Strain-Induced Crystallization of the NR Composites

Composite	C_1 (MPa)	C_2 (MPa)	α_u	Bound rubber (%)
NR/N330	0.822	0.360	2.48	19.1
NR/N330/N770	0.748	0.279	2.53	8.6
NR/N770	0.614	0.255	2.74	3.6

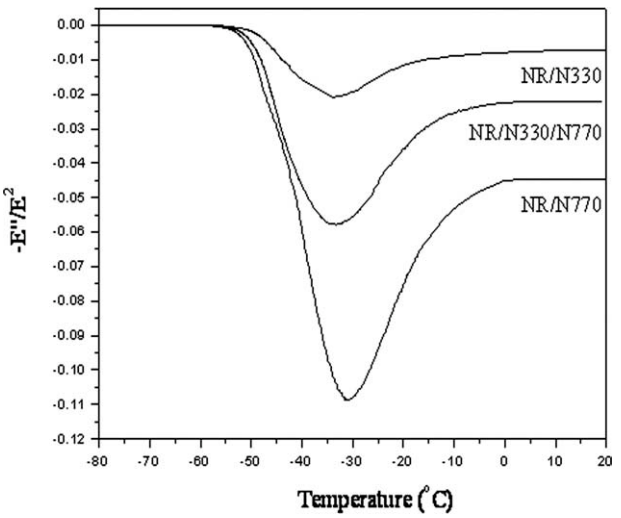

Figure 7 Dependence of the viscoelastic properties on the temperature (E is the viscoelastic modulus).

amplification effect of the filler is strengthened. Table V shows that the NR/N330 composite had the largest content of bound rubber; thus, during the stretching course of the cyclic loading, the strain-induced crystallization in the crack tip of the N330-filled rubber could have occurred much earlier, and the crystallinity should have been greater; this led to an increase in the crack-growth resistance, in accordance with the experimental results of the crack-growth testing, in which the N330-filled rubber showed the lowest crack-propagation velocity at a given value of T. On the other hand, because of its lowest content of bound rubber, its largest onset strain of strain-induced crystallization, and accordingly, its lower crystallinity, the rubber filled by N770 displayed the worst crack-growth resistance, as shown in Figure 2. A more detailed and direct investigation of these relations is being carried out with the help of X-ray diffraction and will be published elsewhere.

The resistance of crack growth is also dependent on the viscoelastic property of rubber matrix, which is the other contribution to T and is largely affected by the inclusion of fillers. According to the theory reported by Persson and Brener,[31] the tearing energy at crack rate v [$T(v)$] can be expressed by

$$T(v) = T_0\left[1 - \frac{2}{\pi}E_0\int_0^{2\pi v/a} d\omega \frac{F(\omega)}{\omega}\mathrm{Im}\frac{1}{E(\omega)}\right]^{-1} \quad (16)$$

where E_0 is the modulus in the outer region of the crack tip (considered the rubbery region); a is the crack tip diameter; ω is the perturbing frequency, which is defined as v/r (where r is the distance from the crack tip); $F(\omega)$ is equal to $[1 - (\omega a/2\pi v)^2]^{1/2}$; Im$[1/E(\omega)]$ denotes the imaginary part of $1/E(\omega)$; and $E(\omega)$ is the viscoelastic modulus, which is given by $E(\omega) = E' + iE''$ (where E' is the storage modulus and E'' is the loss modulus). Thus, the following expression can be deduced with some mathematics and transforms to

$$\mathrm{Im}\frac{1}{E(\omega)} = -\frac{E''}{E(\omega)^2} \quad (17)$$

On the basis of eqs. (9) and (10), $T(v)$ increases with increasing values of $-E''/E(\omega)^2$. Because of the time–temperature superposition, the variation of $E(\omega)$ with frequency can be replaced by the relationship between $E(\omega)$ and temperature. Figure 7 shows the dependence of values of $-E''/E(\omega)^2$ on temperature. Obviously, the N330-filled rubber had the largest values of $-E''/E(\omega)^2$; therefore, $T(v)$ of the N330-filled NR was the largest among the three kinds of rubber composites; this indicated that NR reinforced by N330 needed more energy dissipation at the same crack-growth velocity during the cyclic loading compared to the other two rubbers. That is, the ability of the crack-growth resistance was enhanced. On the contrary, NR reinforced by N770, which had the lowest values of $-E''/E(\omega)^2$, had the worst resistance to crack growth. In conclusion, because both contributions of NR filled with N330 correlated with T were most remarkable, it had the strongest resistance to crack growth compared with the other two rubber composites.

CONCLUSIONS

The addition of carbon black changed the viscoelastic properties, local deformation, and strain-induced crystallization of rubber, all of which greatly influenced the crack-growth behavior. The N330-filled NR possessed the lowest values of crack growth at a given value of T, namely, the strongest resistance to crack growth, whereas N770-filled NR had the worst crack-growth resistance. The studies on the Mullins and Payne effects showed highest filler–filler and rubber–filler interactions and the largest energy dissipation during cyclic loading in the NR/N330 composite, which induced the strongest crack-propagation resistance. Because the largest amount of bound rubber existed in NR filled with N330, this compound exhibited the earliest appearance and strongest ability of crystallization, which led to the most powerful resistance to crack growth at a given value of T compared with rubbers filled with other carbon blacks. The study on the viscoelastic properties by DMA confirmed that the NR/N330 composite had the largest viscoelastic contribution in the viscoelastic region in the front of the crack tip. This

further validated the best endurance to fatigue crack propagation of the NR filled with N330.

The authors appreciate Yan Liu and Zhenghong Wang for their great help with the fatigue testing.

References

1. Yang, Q. Z. Modern Rubber Techniques; Sinopek: Beijing, 2004; p 155.
2. Mars, W. V.; Fatemi, A. Int J Fatigue 2002, 24, 949.
3. Griffith, A. A. Philos Trans A 1920, 221, 163.
4. Thomas, A. G. J Polym Sci 1958, 31, 467.
5. Lake, G. J.; Lindley, P. B. J Appl Polym Sci 1965, 9, 1233.
6. Dizon, E. S.; Hicks, A. E.; Chirico, V. E. Rubber Chem Technol 1974, 47, 231.
7. Kim, J. H.; Jeong, H. Y. Int J Fatigue 2005, 27, 263.
8. Lake, G. J.; Lindley, P. B. Rubber J 1964, 146, 30.
9. Chung, B.; Funt, J. M.; Ouyang, G. B. Rubber World 1991, 204, 46.
10. Westermann, S.; Kreitschmann, M.; Pyckhout-Hintzen, M.; Richter, D.; Straube, E. Phys B 1997, 234, 306.
11. Heinrich, G.; Vilgis, T. A. Macromolecules 1993, 26, 1109.
12. Wang, M. J. Rubber Chem Technol 1998, 71, 520.
13. Chenal, J. M.; Gauthier, C.; Chazeau, L.; Guy, L.; Bomal, Y. Polymer 2007, 48, 6893.
14. Schubel, P. M.; Gdoutos, E. E.; Daniel, I. M. Theor Appl Fract Mech 2004, 42, 149.
15. Leblanc, J. L.; Hardy, P. Kautsch Gummi Kunstst 1991, 44, 1119.
16. Lake, G. J. Rubber Chem Technol 1995, 68, 435.
17. Lindley, P. B. Int J Fract 1973, 9, 449.
18. Kraus, G. J Appl Polym Sci 1984, 39, 75.
19. Zhu, Z. Y.; Thompson, T.; Wang, S. Q.; von Meerwall, E. D.; Halasa, A. Macromolecules 2005, 38, 8816.
20. Bokobza, L. Macromol Mater Eng 2004, 289, 607.
21. Bueche, F. J Appl Polym Sci 1961, 5, 271.
22. Persson, B. N. J.; Albohr, O.; Heinrich, G.; Ueba, H. J Phys: Condens Matter 2005, 17, 1071.
23. Lee, D. J.; Donovan, J. A. Rubber Chem Technol 1987, 60, 910.
24. Trabelsi, S.; Albouy, P. A.; Rault, J. Macromolecules 2002, 35, 10054.
25. James, H. M.; Guth, E. J Chem Phys 1943, 11, 4545.
26. Furukawa, J.; Onouchi, Y.; Inagaki, S.; Okamoto, H. Polym Bull 1981, 6, 381.
27. Pradhan, S.; Costa, F. R.; Wagenknecht, U.; Jehnichen, D.; Bhowmick, A. K.; Heinrich, G. Eur Polym J 2008, 44, 3122.
28. Poompradub, S.; Tosaka, M.; Kohjiya, S.; Ikeda, Y.; Toki, S.; Sics, I.; Hsiao, B. S. J Appl Phys 2005, 97, 103529.
29. Dannenberg, E. M. Rubber Chem Technol 1986, 59, 512.
30. Starr, F. W.; Schrøder, T. B.; Glotzer, S. C. Macromolecules 2002, 35, 4481.
31. Persson, B. N. J.; Brener, E. Phys Rev E 2005, 71, 036123.